

Saponite Nanoclay Based Plasticized PVDF-CO-HFP /LithiumBis(Perflouro Methane Sulfonyl)Imide Composite Electrolytes for Li-ion Batteries

¹Carol Stanly Semler, ²Mohamed Tharik, ³Palaniswamy Vickraman, ⁴Natarajan Kirubanand

¹Research Scholar, ²Research Scholar, ³Professor, ⁴Research Scholar

¹ Department of physics,

¹Gandhigram Rural Institute (Deemed to be University), Gandhigram, Dindigul, Tamil Nadu, India

Abstract : In the present study smectites family of phyllosilicates, the Saponite nano clay (<80nm) effect as a filler in consonance with EC: DMC (1:1) v/v ratio on PVdF-co-HFP – LiBETI matrix has been investigated by a.c impedance, XRD and FT-IR vibrational spectroscopy. The ionic conductivity of the order of 10^{-7} - 10^{-5} S cm^{-1} has been observed at the minimal participation of clay platelets than its huge presence of the non-polar phase of the PVdF has been considerably suppressed as noted XRD. The vibrational bands of characteristics PVdF crystal have gone in intensity variations very doublets with increase in clay particulates suggestive of the metal complex formation within has been observed.

IndexTerms – Li-ion Batteries, Polymer Composite Electrolytes, Saponite Nanoclay, PVDF.

I. INTRODUCTION

Lithium rechargeable batteries have been progressing for the last three decades with lot of innovations with their fullest capacity as energy storage devices in portable and electric vehicles [1]. Among the three important components of lithium battery such as anode, cathode and electrolytes, the research on electrolyte component has gone different explorations with reference to the compatibility with electrodes and safety concerns during charging and discharging and for high ion energy density deliverance. As a result the solid polymer electrolytes (SPEs) have been found as an alternative to the liquid electrolyte [2].

Although comprehensively solid polymer electrolytes (SPEs) have accomplished certain safety measurements the ionic conductivity of them have not been appreciably improved. These drawbacks have been circumvented with the use of Gel polymer electrolytes (GPEs) (the cations are trapped in the liquid cavities) [3, 4]. Albeit the considerable progress of ionic conductivity of GPEs, the concentration of Li^+ cations has not been sufficient due to ion-pair formation. To curb the ion-pair formation and cornering the anions and having the ionic conduction through single cationic movements, these GPEs have been dispersed with layered silicates. Hitherto layered silicates in nano size have been investigated as fillers in GPEs. The layered structure of nanoclay allows for the intercalation of the polymeric chains between the layers, thereby reducing the crystallinity of the GPEs and thus enhancing its conductivity and compatibility with lithium electrodes [5-7].

2 MATERIALS AND METHODS

2.1 MATERIALS

Poly(vinylidene fluoride) (PVDF) with 12 mol% of hexafluoro propylene (HFP) has supplied by Solvay (solexis), France with trade name solef of molecular weight 5.34×10^5 g/mol was used. The plasticizers ethylene carbonate (EC) and dimethyl carbonate (DMC) were obtained from Aldrich, USA and used as such. The Saponite particle size <80nm and molecular weight 480.19 g/mol, purchased from Nanoshel LLC, Intelligent materials pvt. Ltd. The solvent tetrahydrofuran (THF), HPLC grade was purchased from E. Merck, India and used without further purification. Lithium bis(perfluoroethanesulfonyl) imide (BETI) of molecular weight 387.13g/mol was purchased from Fluka, USA and used as received. Polymer NanoClay Composite Electrolytes (PNCCEs) (membranes) were prepared as per the composition given Table 1 by solution casting technique.

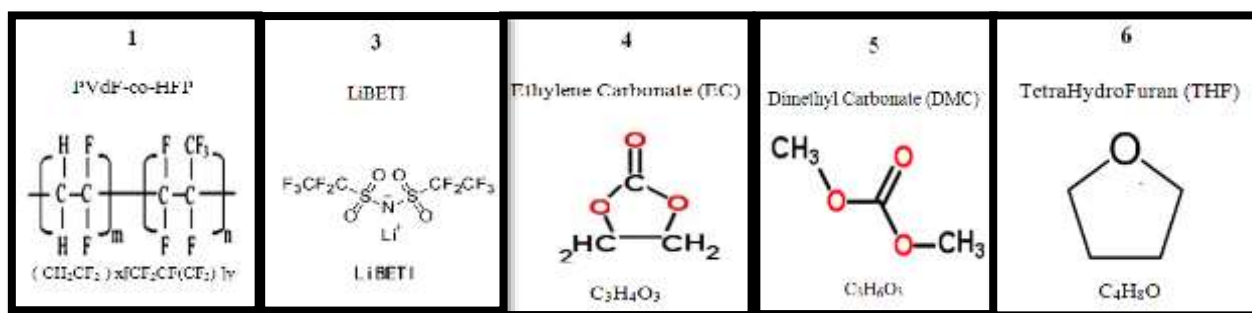
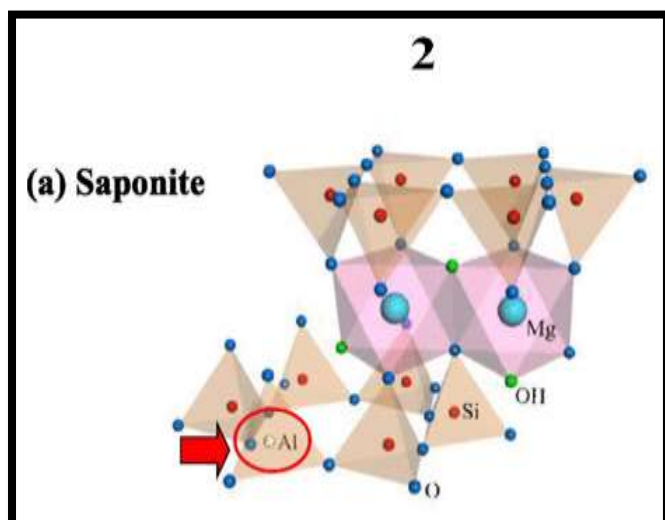


Fig. 1 Materials Structure

SAPONITE NANOCLAY:

Saponite^[8], a trioctahedral member of the smectite family, is built from two SiO_4 tetrahedral layers and one MgO_6 octahedral layer arranged in a TOT sandwich (T = SiO_4 tetrahedral layer and O = MgO_6 octahedral layer). Substitution of Si by Al in the tetrahedral layer creates a negative charge which is compensated by cations such as Na^+ located in the interlayer space.



Purity	: 99%
Particle size	: <80 nm
Purchase	: Nanoshel LLC
SiO_2	: 37.54%
Al_2O_3	: 10.62%
Fe_2O_3	: 11.2%
Na_2O	: 0.68%
CaO	: 1.17%
MgO	: 18.89%
H_2O	: 18.76%
All Other Metal	: <0.1 %

Fig.2 Saponite Structure

2.2 SAMPLE PREPARATION

The preparation of PNCCEs has been carried out using solution casting technique. The required quantities of polymer, filler, salt and plasticizer in wt% shown in Table 1 were mixed in a common solvent tetra hydro furan (THF). The ingredients were allowed to fully disperse and swell requires 24hrs. After 24 hrs the particular composition of the every solution had been sonicated for 15 – 30 minutes, in order to ensure high homogeneity of solution. Immediately after the sonification, the stock solution of particular composition had been stirred and monitored at room temperature till the formation of viscous solution was obtained. The semisolid viscous solution was poured onto circular petty dishes, so as to evaporate the THF. Complete drying had taken place about 48 – 78 hrs. The peeled off free standing films were incubated in vacuum oven at 100°C with the pressure of 10^{-5} to further remove some traces of solvent. Thus the complete free standing films as prepared were kept in vacuum controlled desiccator for further characterization studies.

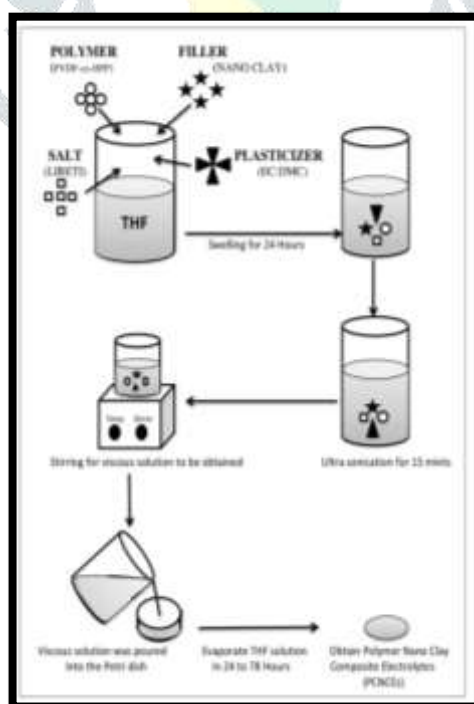


Fig. 3. Sample preparation Technique

2.3 METHODS

Ionic conductivities of PNCCEs were studied by using HIOKI 3532-50 LCR Hi-tester in the frequency range 50 Hz - 5MHz with conductivity cell consisting of two circular stainless steel blocking electrodes (SS/PNCCEs/SS) of 1cm² cross-sectional area. FTIR spectra of PNCCEs were recorded using perkinelmer/spectrum 2 spectrophotometer in the wave number range from 4000 to 400 cm⁻¹ at a resolution of $\pm 5\text{cm}^{-1}$. XRD analysis was carried out to investigate the crystalline nature of PNCCEs using a PAN-Analytical X'PertPRO powder X-ray Diffractometer Cu K α ($\lambda=1.54060\text{ \AA}$), over the range of $2\theta=10^\circ\text{--}80^\circ$ at 25°C temperature.

3 RESULT AND DISCUSSION

3.1 IONIC CONDUCTIVITY STUDIES

PVdF-co-HFP/LIBETI/SAPONITE:EC:DMC composite electrolytes (PNCCEs) SAP

The ac. impedance measurement on polymer nanoclay composite electrolytes (PNCCEs) membranes has been carried out by sandwiching them in between the two stainless steel electrodes otherwise known as blocking electrodes constitutes electrochemical cell arrangement at various frequencies ranging from 50 Hz - 5 MHz. The Nyquist plot, a kind of a plot is used for evaluating A.C impedance data in this dissertation.

Thus A.C impedance studies begin by considering the blocking electrode setup. An A.C voltage is applied to the cell and the frequency is varied. The equivalent circuit representing the A.C response of the cell is shown in Fig. 4. The electrodes become alternatively positively and negatively charged and the alternating field across the electrolyte causes the lithium ions to migrate back and forth in phase with the voltage. The migration of the lithium ions is represented by the resistor R_g . At the same time, the immobile polymer chains become polarized in the alternating field, just as they would if the polymer film were devoid of mobile charges and, this dielectric polarization may be represented by a capacitor C_b .

$$C_b = \frac{\epsilon \epsilon_0 A}{l}$$

The bulk polarization and ionic migration are physically in parallel therefore their representative components, R_b and C_b , are connected in parallel, both are in series with the electrode capacitance C_e . For a cell with electrode separation $l=1\text{ cm}$, and electrode area $A=1\text{cm}^2$, the bulk and electrode capacitances are typically $\approx 10^{-12}$ and 10^{-6} F respectively. C_b is simply related to the dielectric constant of polymer. Since C_e is in series with the parallel combination of R_b and C_b , the equation for the total impedance is obtained simply by adding the impedance of the capacitor C_e to that of the parallel RC combination as derived.

$$Z_{total}^* = R_b \left[\frac{1}{1 + (\omega R_b C_b)^2} \right] - j \left(R_b \left[\frac{\omega R_b C_b}{1 + (\omega R_b C_b)^2} \right] + \frac{1}{\omega C_e} \right)$$

The complex impedance plot predicted by this equation is given in fig.3.4. Because of the frequency – dependent impedance of capacitor, the full equivalent circuit of fig.3.4. reduces to simpler equivalent circuits over limited frequency ranges. At the high frequencies, when the impedance of the bulk resistance and capacitance are of the same magnitude $1/\omega C_b \approx R_b$ both the bulk resistance and capacitance contribute significantly to the overall impedance whereas the impedance of the electrode capacitance, C_e , is insignificant ($C_e \approx 10^6 C_b$). Therefore at high frequencies the equivalent circuit reduces to a parallel $R_b C_b$ combination which gives rise to the semicircle in the complex impedance plane. At low frequencies $1/\omega C_b \ll R_b$ and hence C_b makes a negligible contribution to the impedance, the equivalent circuit thus reduces to a series combination of R_b and C_e appearing as a vertical spike displaced a distance R_b along the real axis. At very low frequencies the equivalent circuit would simply to the electrode capacitance C_e only.

It generally true that the high-frequency response yield information about the properties of the electrolyte. For example, the high-frequency semicircle yields the bulk resistance R_b and, knowing R_b and ω_{max} , the bulk capacitance, C_b , from $\omega_{max} R_b C_b = 1$. The low-frequency response on the other hand carries information on the spike, $C_e = 1/Z\omega$. Overall, the magnitude of all the fundamental electrical properties of the cell may be obtained from the complete impedance data. In particular, R_b is the effective d.c. resistance of the electrolyte, therefore simply by sandwiching a polymer electrolyte between two blocking electrodes, the d.c. conductivity of the electrolyte may be very easily determined^[9].

The ionic conductivities of the PNCCEs with reference to the composition code with SAP 1, SAP 2, SAP 3, SAP 4 and SAP 5 have been examined (Table 1). When **Saponite** nanoclay and Lithium bis(perfluoro ethane sulfonyl) imide are dispersed in equal proportion without EC: DMC with polymer(SAP 3) showed PNCCEs (SAP 3) conductivity order of 10^{-7} Scm^{-1} . But when EC is added SAP 4 it has shown improved conductivity of one order. When DMC is added (SAP 5) further enhancement in the order of conductivity 10^{-5} Scm^{-1} is noted. It is clearly observed that the role of plasticizers and their participation have clearly enhanced conductivity reveals that the plasticizer could well dissociate the LiBETI salt into its fragment cations and anions. These free ions are never allowed to form ion-pair formation by the **Saponite** nanoclay with its charged surface interaction with the polar host matrix is noted^[10].

The observation of ionic conductivity variations have also been examined by varying ratio of filler: plasticizer (Table 1) with the sample codes SAP 6 to SAP 11. The sample SAP 6, (free from filler content but the maximized plasticizer content) gives the conductivity in the order of 10^{-5} Scm^{-1} but when the **Saponite** nanoclay is added to the minimum content of 1.5wt% (SAP 7) (with proportionate decrement in the plasticizer content), improved the magnitude of conductivity. The subsequent addition of nanoclay insteps of 1.5wt% increment with proportionate corresponding decrement in plasticizer has however not shown enhanced conductivity rather drastically reduced the conductivity in the order of 10^{-6} Scm^{-1} . The conductivity measurement on these PNCCEs (SAP 6 to SAP 10) have well suggestive of the minimal participation of nanoclay dispersoids have significantly improving /providing better path channels for Li cation migration resulting the conductivity is observed^[11].

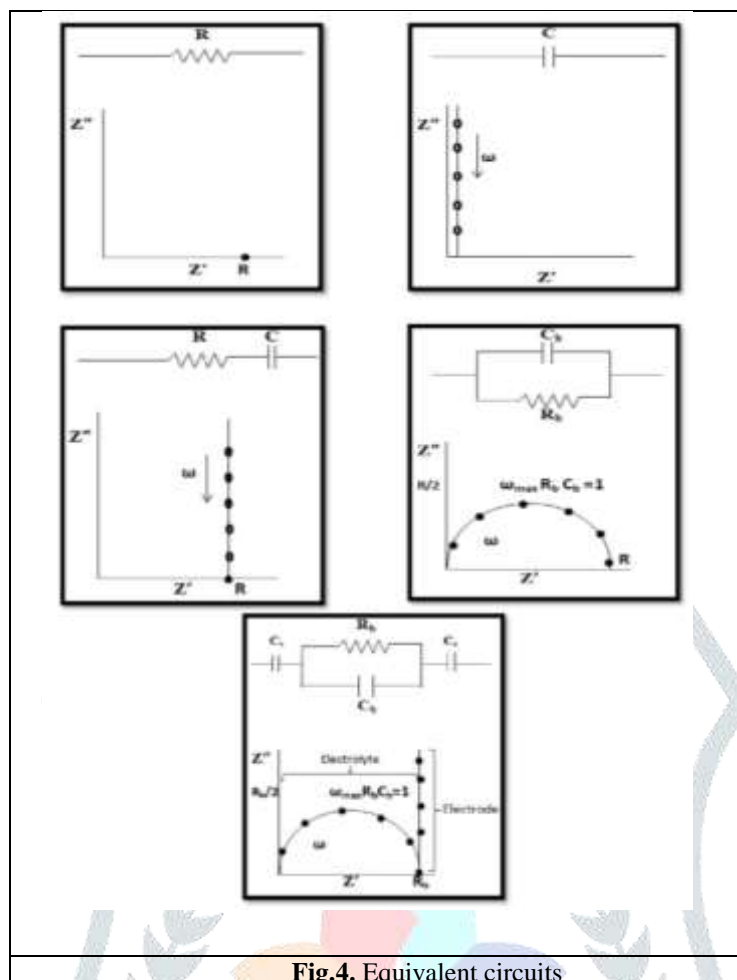


Fig.4. Equivalent circuits

Table 1: Composition and ionic conductivity of PNCCEs

SAMPLE CODE	PVdF-co-HFP wt%	SAPONITE wt%	LIBETI wt%	EC : DMC wt%	IONIC CONDUCTIVITY S _{cm} ⁻¹
SAP 1	25	0	0	0 : 0	—
SAP 2	25	5	0	0 : 0	—
SAP 3	25	5	5	0 : 0	8.31X10 ⁻⁷
SAP 4	25	5	5	35 : 0	4.16X10 ⁻⁶
SAP 5	25	5	5	32.5 : 32.5	1.35X10 ⁻⁵
SAP 6	25	0	5	35 : 35	2.86X10 ⁻⁵
SAP 7	25	1.5	5	34.25 : 34.25	2.77X10 ⁻⁵
SAP 8	25	3	5	33.5 : 33.5	7.93X10 ⁻⁶
SAP 9	25	4.5	5	32.75 : 32.75	3.019X10 ⁻⁶
SAP 10	25	6	5	32 : 32	6.08X10 ⁻⁶
SAP 11	25	7.5	5	31.25 : 31.25	8.53X10 ⁻⁶

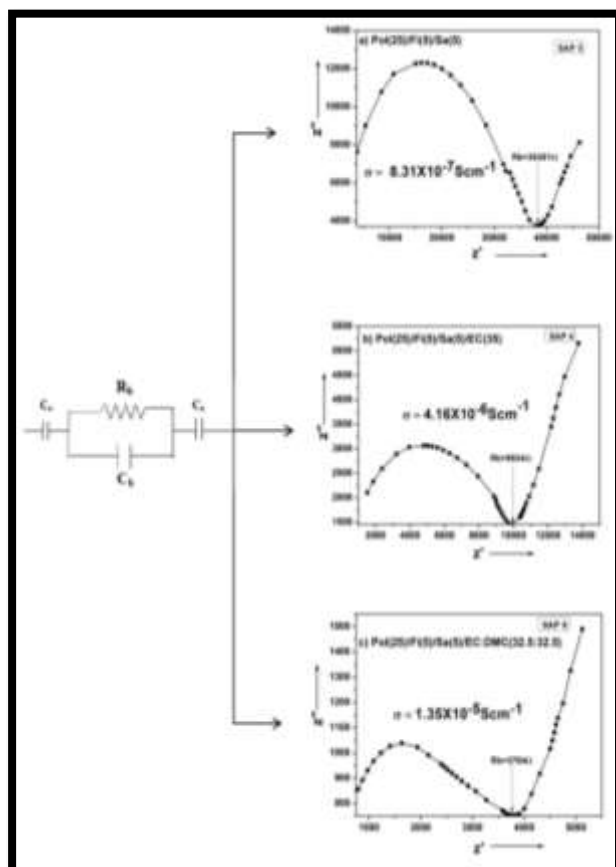


Fig 5. A.C impedance Studies of a) SAP 3, b) SAP 4, c) SAP 5

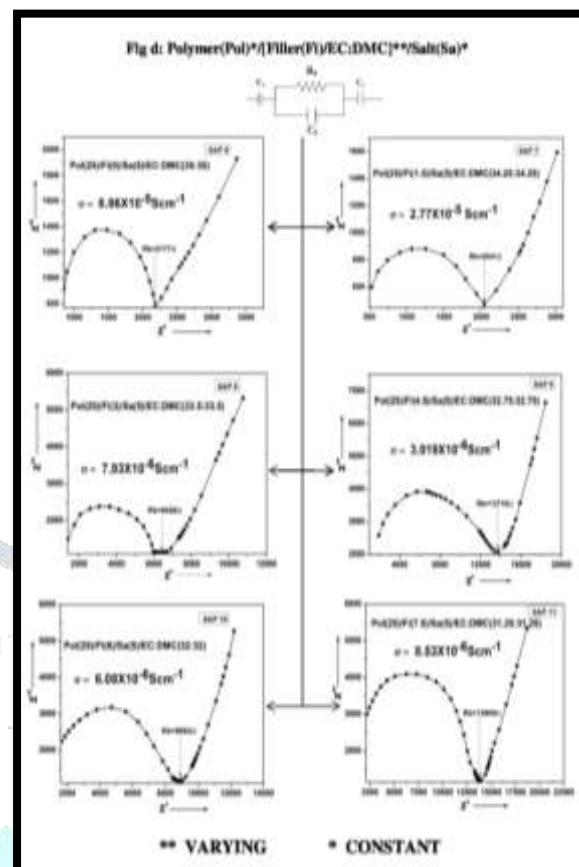
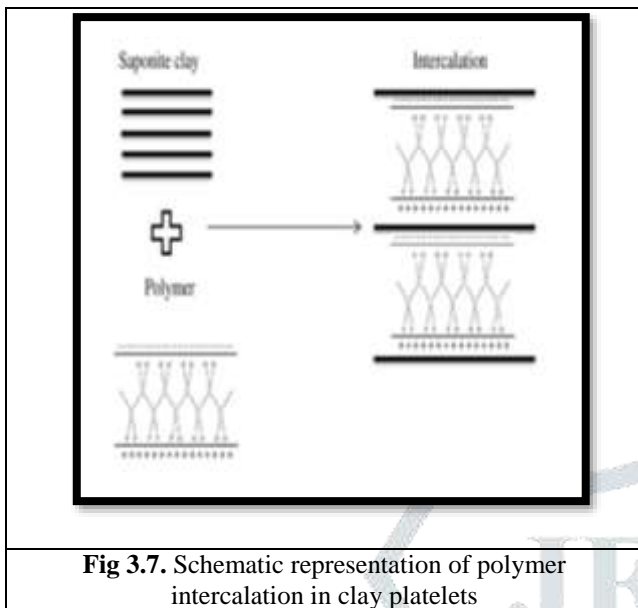


Fig 6. A.C impedance Studies of SAP 6, SAP 7, SAP 8, SAP 9, SAP 10 and SAP 11

In this work different clays in nano less than or equal to <80 nm have been dispersed as a solid plasticizers to dissociate electrolyte into lithium (Li^+ /cations) and Li^- anions gives rise to no. of charge carriers and also facilitating their mobility through the process called intercalation and exfoliation. In the intercalation process, the gallery spacing between the layered silicates due to the protrusion of chain molecules of PVdF widened. This widening and the interaction between the polar group of the polymer and the charge effects of the surface clays provides pathway for the lithium (Li^+) cations for gaining momentum provides the mobility and as a result ionic conductivity variations are observed. On the other hand in the exfoliation process, due to the increase in the concentration of clay platelets, in the present study 3wt%, 4.5wt%, 6wt% and 7.5wt% their distorted intercalation or exfoliation takes place wherein the PVdF molecules have coiled down the layered sheets and distorting them in such a way that the Li^+ cations thus generated in our case 1.5wt% are have been masked or constricted their movement result in decrementing ionic conductivity.

Thus the intercalation and exfoliation are said to be phenomena of interaction between layered silicates and the polar polymers PVdF interactions between them have showed the polymers nano composite clay electrolytes change in their crystallinity and amorphousity. The crystallinity and amorphousity of the membranes have been subjected to XRD studies by varying the compositional dependence of plasticizer and clay concentration. In general plasticizer when it is added with the polymer, it gives rise to the flexibility to the polymer chains enabling Li^+ cations transit by hopping mechanism through the end points of chain segments. In our case, the plasticizer are used to do the process of flexing the polymer host as well as dissolving Li^+ salts for generating charge carriers for conductivity and converting certain crystallites phase of PVdF into amorphous phase. In this study the plasticizer rich phase with clay poor phase have not profusely changed their intensity of their characteristics phases of PVdF and the filler rich phase with poor plasticizer phase have also not contributed much in the change of phase of PVdF.



3.2 XRD STUDIES

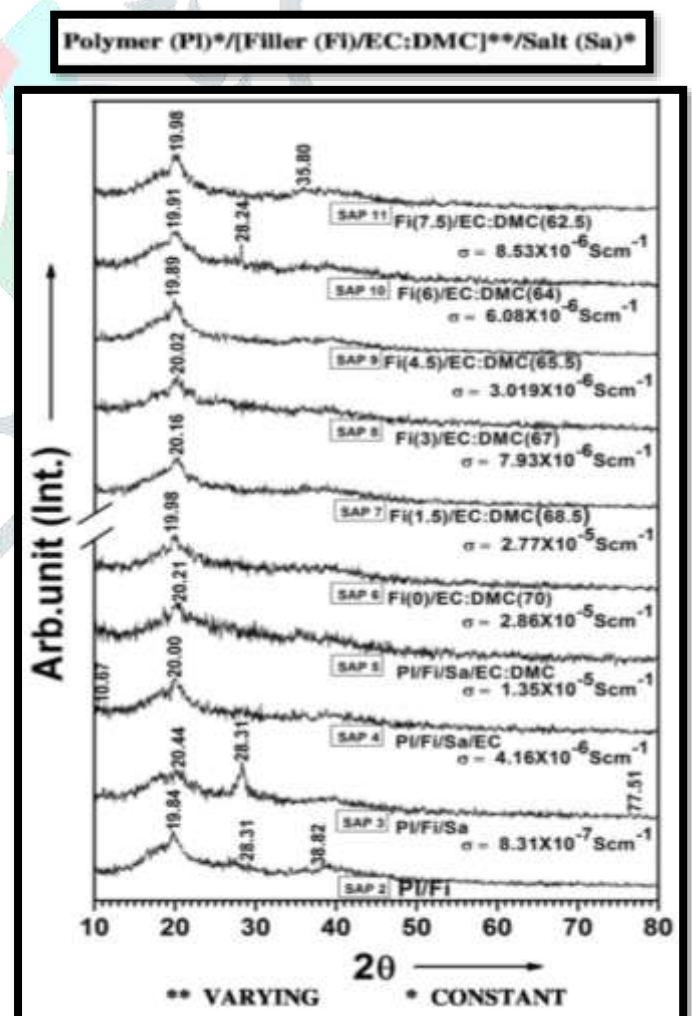
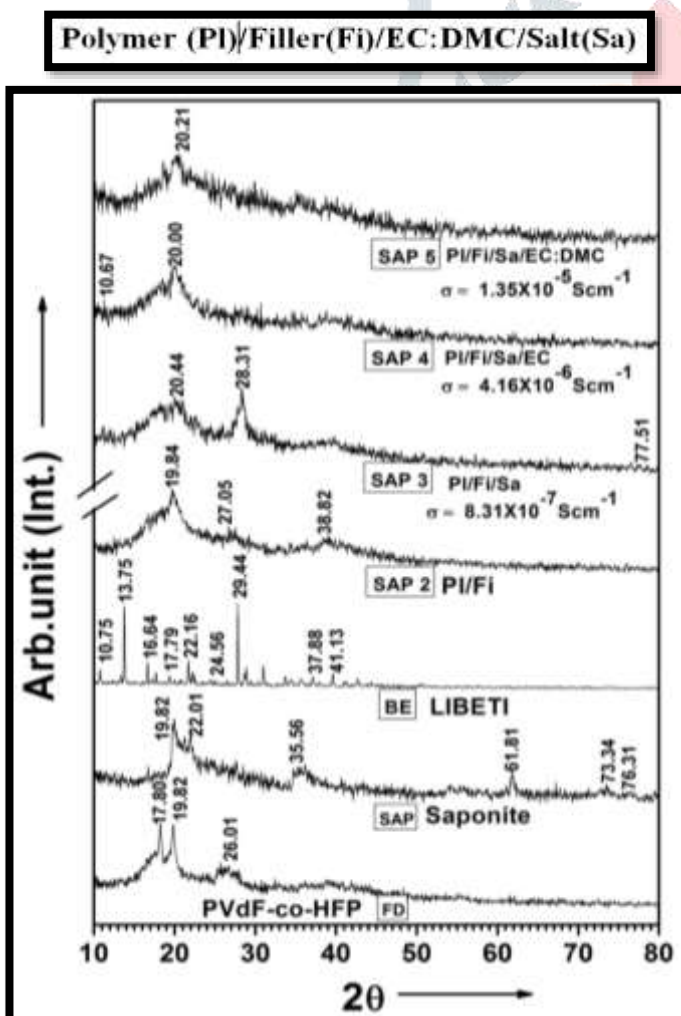


Fig 8. XRD diffractogram of FD, SAP, BE, SAP 2 and PNCCEs

Fig 9. XRD diffractogram of PNCCEs SAP 2, SAP 3, SAP 4,

Table 2: Composition and XRD peak appearance of PNCCEs

(SAP 3, SAP 4, SAP 5)

SAP 5, SAP 6, SAP 7, SAP 8, SAP9, SAP 10 and SAP 11



SAMPLE CODE	PVdF-co-HFP wt%	SAPONITE wt%	LIBETI wt%	EC : DMC wt%	XRD 2 θ in degree	
					10 $^{\circ}$ – 20 $^{\circ}$	20 $^{\circ}$ -40 $^{\circ}$
SAP 1	25	0	0	0 : 0	17.80(110- α) 18.24(020- α) 19.8(110- α)	26.01(021- α)
SAP 2	25	5	0	0 : 0	19.84(110- α)	27.05(021- α) 38.82(021- α)
SAP 3	25	5	5	0 : 0		20.44(110- α + γ) 28.31(110- α)
SAP 4	25	5	5	35 : 0	10.67	20.00(020- α)
SAP 5	25	5	5	32.5 : 32.5		20.21(110- α + γ)
SAP 6	25	0	5	35 : 35	19.98(110- α)	
SAP 7	25	1.5	5	34.25 : 34.25		20.16(110- α)
SAP 8	25	3	5	33.5 : 33.5		20.02(020- α)
SAP 9	25	4.5	5	32.75 : 32.75	19.89(110- α)	
SAP 10	25	6	5	32 : 32	19.91(110- α)	28.24
SAP 11	25	7.5	5	31.25 : 31.25	19.98(110- α)	35.80(γ -phase)

3.3 FT-IR STUDIES

The vibrational spectroscopy as a tool is used to understand the molecular interaction of various constituents of the as prepared PNCCEs in the wave number region 400-3000 cm^{-1} . As the initial step, pristine PVdF-co-HFP supplied by the Solvay solexis France, has been recorded in 400 – 3000 cm^{-1} . The characteristic peaks associated with the pristine are observed at 488 cm^{-1} (sharp), 610 cm^{-1} (medium sharp), 759 cm^{-1} (medium distinct singlet) strong sharp peak 874 cm^{-1} are noted correspond to α -phase VdF crystallites. Further doublet formation one at 1068 cm^{-1} (very weak in appearance) co-folded with 1179 cm^{-1} (very strong) correspond to C-F grouping [16, 17], the methylene group CH₂ bending is noted at 1396 cm^{-1} .

The characteristics peaks of PVdF-co-HFP noted in the previous paragraph have shown shift in wave number and their intensity variations after adding **Saponite** clay are noted appeared and located at 460 cm^{-1} , 610 cm^{-1} drastically reduced in its envelope and 759 cm^{-1} shifts to 877 cm^{-1} with improved intensity contour and 874 cm^{-1} shifts to 835 cm^{-1} and well patterned 1068 cm^{-1} and 1179 cm^{-1} doublet correspond C-F grouping, 1068 cm^{-1} has appeared in enhanced intensity and co-folded well with 1172 cm^{-1} are well illustrative of C-F grouping hindrance arising due to charged platelets of clay interaction. The CH₂ bending shifts to 1399 cm^{-1} from 1396 cm^{-1} shows clay dispersion less pronounced with it.

These typical enhancements in intensity envelopes with shifts in bands in characteristic VdF crystalline phases as attributed as per the literature [18] again undergoes distinct intensity variations as well as bands shift by adding LiBETI as noted ie. 488 cm^{-1} (pure PVdF) band broadening still broadened and found at 480 cm^{-1} in (SAP 3) but in contrast 610 cm^{-1} medium sharp (SAP 1) contrast drastic reduction in SAP 2 in considerably grown with pronounced presence suggestive of salt interaction with so called polymer + **Saponite** clay intercalation. On the other hand 759 cm^{-1} /875 cm^{-1} appears at 877 cm^{-1} /835 cm^{-1} reappears as such with no change in intensity as well as their location noted and the same way well grown 1068 cm^{-1} in SAP 2 once again drastically return its presence, however, may be its co-folding with 1172 cm^{-1} . When SAP 3 is plasticized with EC, 480 cm^{-1} shifts to 472 cm^{-1} (medium), new appearance of 724 cm^{-1} /778 cm^{-1} distinctly grown with very short traces as attributed to EC present. The strong α phase of PVdF crystals at 877 cm^{-1} /835 cm^{-1} appeared as such and doublet at 1075 cm^{-1} /1169 cm^{-1} CF grouping intensity have grown due to the interaction of EC is noted, the C=O carbonyl band has been at 1637 cm^{-1} and 1776 cm^{-1} as sharp/medium bands. When DMC is added to the PVdF-co-HFP/**Saponite**/LiBETI/EC composite 724 cm^{-1} and 778 cm^{-1} reappeared and kink like appearance in SAP1, SAP 2, SAP 3, SAP 4 appeared in well grown distinct presence explores 513 cm^{-1}

of β phase of VdF crystals suggestive of nucleation of VdF crystals and transform certain crystallites to β phase (polar nature) is well noted but in sample SAP 6, no trace of **Saponite** clay not nucleating its presence is noted. The kink like appearance in SAP 5 at 809 cm^{-1} has grown as a distinct peak in SAP 6 at 976 cm^{-1} suggestive of role of clay intercalation with polar group of PVdF is evidenced. However highly loading of clay from 4.5wt%, 6.0wt%, 7.5wt% C-F grouping appearance /reappearance are well illustrating steric hindrance and imbalance of confirmed physical orientation of VdF crystallites are well understood. It is noted that at high loading of **Saponite** exfoliates the β phase of VdF crystals (513 cm^{-1}) is very suggestive of polar – polar interaction of charged platelets of **Saponite** with change in galleries spacing widening with fluorine domain confirm degree of complexation of the clay particulates correspond of poor/rich phase of plasticizer are observed.

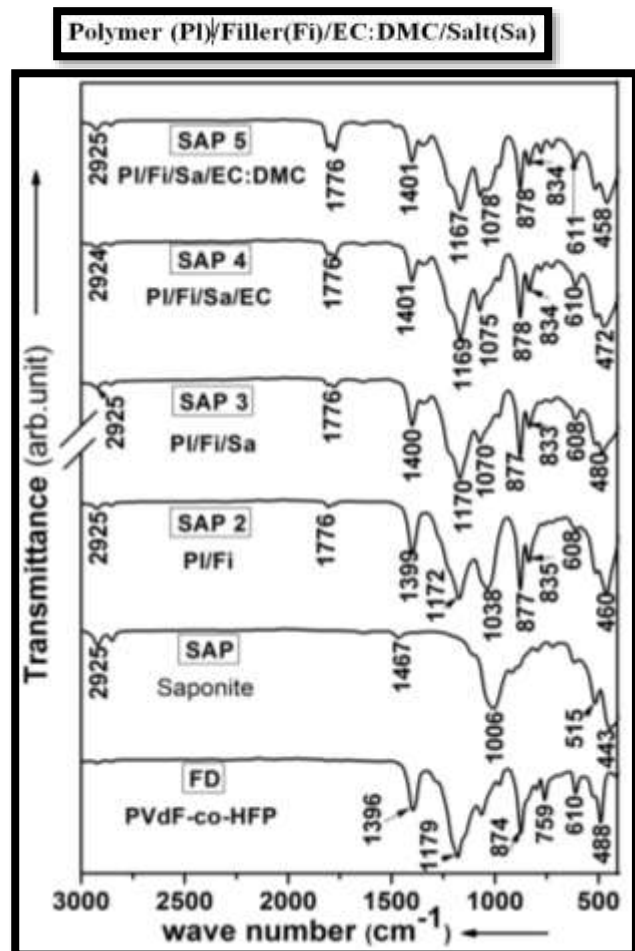


Fig 10. FT-IR studies on FD, SAP, SAP 2 and PNCCEs (SAP 3, SAP 4, SAP 5)

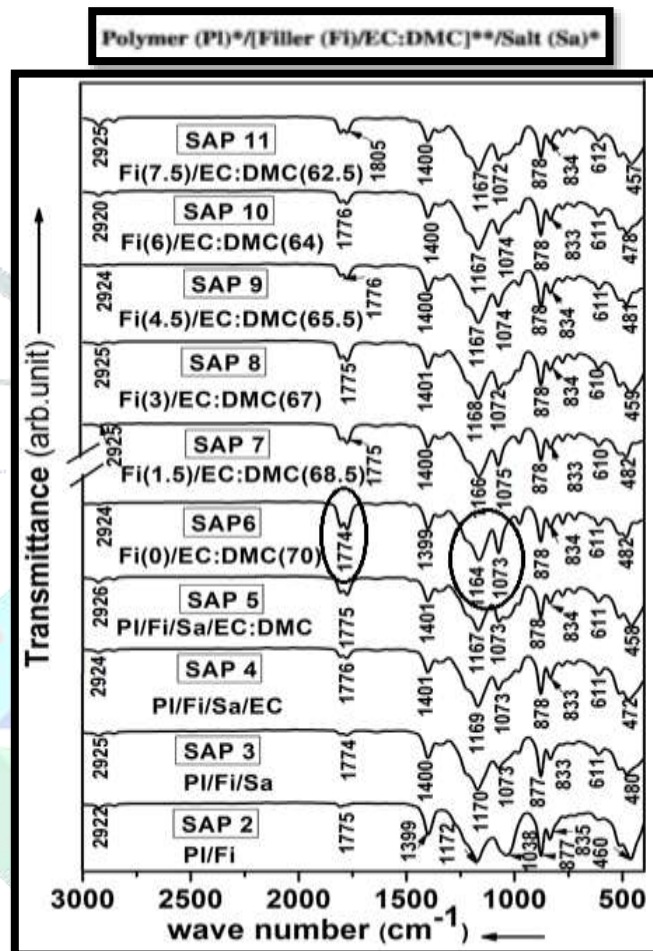


Fig 11. FT-IR studies on PNCCEs SAP 2, SAP 3, SAP 4, SAP 5, SAP 6, SAP 7, SAP 8, SAP 9, SAP 10 and SAP 11

The C=O carbonyl band enshrouded EC/DMC ring breaching appearance with enhanced intensity in **Saponite** clay free membrane is started to reduce in intensity with consistent increases of clay platelets suggestive of plasticizer clay intercalation and dominance of clay platelets with polymer interaction than with plasticizer dissolution noted.

Wave Number Cm ⁻¹	SAP 1	SAP 2	SAP 3	SAP 4	SAP 5	SAP 6	SAP 7	SAP 8	SAP 9	SAP 10	SAP 11
Medal Oxide Region											
400	438	480	472	458	482	482	459	481	478	457	
500											
600	610	611	611	611	611	610	610	611	611	612	612
Finger Print Region											
700											
800	835 877	833 878	834 878	834 878	834 878	833 878	834 878	834 878	833 878	834 878	834 878
900											
1000	1062	1073	1073	1073	1073	1075	1072	1074	1074	1074	1072
1100	1179	1170	1169	1167	1167	1166	1168	1168	1167	1167	1167
1200											
1300					1399						
1400		1400	1401	1401		1400	1401	1400	1400	1400	1400
1500											
Functional Group Region											
C=O		1774	1776	1775	1774	1775	1775	1775	1776	1776	1805

Table 3.3: Vibrational Bands of PNCCEs

REFERENCES

- [1]. Jin J, Wen Z, Liang X, Cui Y, Wu X, Gel polymer electrolyte with ionic liquid for high performance lithium sulfur battery. Solid State Ionics 225(2012)604–607.
- [2]. Ryou MH, Lee YM, Cho KY, Han GB, Lee JN, Lee DJ, Choi JW, Park JK, A gel polymer electrolyte based on initiator-free photopolymerization for lithium secondary batteries. ElectrochimActa 60:(2012) 23–30.
- [3]. Zhao Y, Zhang Y, Bakenov Z, Chen P, Electrochemical performance of lithium gel polymer battery with nanostructured sulfur/carbon composite cathode. Solid State Ionics 234:(2013) 40–45.
- [4]. Hassoun J, Scrosati B, A high-performance polymer tin sulfur lithium ion battery. AngewChemInt Ed 49:(2010) 2371–2374.
- [5]. Deka M, Kumar, A Electrical and electrochemical studies of poly(vinylidene fluoride)-clay nanocomposite gel polymer electrolytes for Li-ion batteries. J Power Sources 196:(2011) 1358–1364.
- [6]. Shubha N, Prasanth R, Hoon H, Srinivasan M, Dual phase polymer gel electrolyte based on non - woven poly(vinylidene fluoride-co-hexafluoropropylene)-layered clay nanocomposite fibrous membranes for lithium ion batteries. Mater Res Bull 48:(2013) 526–537.
- [7]. Deka M, Kumar, A Enhanced electrical and electrochemical properties of PMMA-clay nanocomposite gel polymer electrolytes. ElectrochimActa 55:(2010) 1836–1842.
- [8]. Liansheng Li, Xinsheng Liu, J Ying Ge, and Ruren Xu, JoHoRocbat and JacekKlinowski, Structural studies of pillared Saponite, J. Phys. Chem. 97, (1993), 10389-10393.
- [9]. MacCallum J.R, Vincent C.A, Polymer electrolytes reviews, Elsevier, New York, 1987. Page no. 248-254.
- [10]. Croce F, Persi L, Scrosati B, Serraino-Fiore F, Plichta E, Hendrickson M.A, Role of the ceramic fillers in enhancing the transport properties of composite polymer electrolytes. Electrochim. Acta 46 (2001) 2457–2461.

- [11]. Hutchison, J.C, Bissessur, R, Shriver, Conductivity Anisotropy of Polyphosphazene–Montmorillonite Composite Electrolytes D. F. Chem. Mater. 1996, 8, 1597-1599.
- [12]. Priya L, Jog J. P, Poly(vinylidene fluoride)/Clay Nanocomposites Prepared by Melt Intercalation: Crystallization and Dynamic Mechanical Behavior Studies Journal of Polymer Science: Part B: Polymer Physics, Vol. 40, (2002) 1682–1689.
- [13]. Zhaohui Li, Guangyao Su, Xiayu Wang, Deshu Gao, Micro-porous P(VDF-HFP)-based polymer electrolyte filled with Al₂O₃ nanoparticles Solid State Ionics 176 (2005) 1903 – 1908.
- [14]. Satapathy. S, Santosh Pawar, Gupta. P K and Varma. K B R, Effect of annealing on phase transition in poly(vinylidene fluoride) films prepared using polar solvent Bull. Mater. Sci., Vol. 34, No. 4, July 2011, pp. 727–733.
- [15]. Kwang Man Kim, Nam-Gyu Park, Kwang Sun Ryu, Soon Ho Chang, Characteristics of PVdF-HFP/TiO₂ composite membrane electrolyte prepared by phase inversion and conventional casting methods Electrochimica Acta 51 (2006) 5636–5644.
- [16]. Silverstein R.M. and Webster F.X, spectroscopic identification of organic compounds, 6th edition., John Wiley and sons, New York, USA, 1997 (chapter 3).
- [17]. Pavia D.L, Lampman G.M. and Kriz G.S, introduction to spectroscopy, Harcourt College publication, USA, 2001 (chapter 1).
- [18]. Li J. C., Wang C. L., Zhong W. L., Zhang P., Wang Q. H., Webb J. F, Vibrational mode analysis of β -phase poly(vinylidene fluoride) Appl Phys. Lett. 81 (2002) 2223.

